

Low-energy differential scattering of electrons and positrons from noble gases

David D. Reid* and J. M. Wadehra

Department of Physics and Astronomy, Wayne State University, Detroit, Michigan 48202

(Received 7 September 1993; revised manuscript received 21 March 1994)

Calculations of cross sections for electron (e^-) and positron (e^+) scattering from ground-state He, Ne, Ar, Kr, and Xe at projectile energies below the lowest inelastic thresholds are presented. The main focus in the present work is on the differential cross sections, since angular distributions depend sensitively on the choice of interaction potentials used in the calculations. A part of the interaction potential used in the calculations includes a parameter-free correlation-polarization potential which is (a) based on physical ideas of what a correlation-polarization potential should be, (b) different for various target gases, and (c) distinct for electron and positron scattering. The present calculations of differential cross sections predict the locations of the principal maxima and minima with good accuracy and the shapes of the calculated differential cross-section curves compare quite well with available experimental cross sections.

PACS number(s): 34.80.Bm

I. INTRODUCTION

The traditional model potential approach, which has been used by a number of investigators, for calculating low-energy electron- and positron-atom elastic-scattering cross sections employs a complex interaction potential that is partitioned into the static, exchange, polarization, and absorption parts. The effects of the correlation between the projectile and the atomic electrons in the near-target region, on the other hand, have been included rather recently [1–5] by using simple parameter-free model potentials. These recent investigations construct a correlation potential (V_{corr}) from the correlation energy functional, which has been constructed both for electrons [6] and for positrons [7]. Our purpose, in the present work, is to obtain a general parameter-free correlation-polarization potential which, when used in the scattering calculations, would provide differential cross sections for the scattering of both electrons and positrons from a large number of target gases over a wide range of impact energies.

We have calculated differential cross sections (DCS) for positron and electron scattering from the rare gases He, Ne, Ar, Kr, and Xe, in the ground state, at energies below the lowest inelastic thresholds for which experimental data are available for comparison; there are no experimental data for positron-helium scattering below the inelastic threshold. For electron scattering, the inelastic thresholds (corresponding to excitation of the target atom) for He, Ne, Ar, Kr, and Xe are 19.8, 16.6, 11.5, 9.9, and 8.3 eV, respectively. For positron scattering, the inelastic thresholds (corresponding to positronium forma-

tion) for He, Ne, Ar, Kr, and Xe are 17.8, 14.8, 9.0, 7.2, and 5.3 eV, respectively. For projectile energies below the inelastic threshold, the interaction potential is real; for electron scattering, it consists of static, exchange, and correlation-polarization parts and, for positron scattering, it has only static and correlation-polarization parts. The static interaction is repulsive for positron-atom scattering and is attractive for electron-atom scattering; thus, apart from an overall sign, the static interaction is the same for electron and positron scattering from a target atom. The correlation-polarization part, on the other hand, is different for the two projectiles since the incident positron correlates differently with the target electrons than the incident electron does. In the present investigations, we propose a new form of the parameter-free correlation-polarization interaction which is based on the correlation potentials V_{corr} of Perdew and Zunger [8] for the electron-scattering calculations and of Jain [4] for the positron-scattering calculations.

Traditionally, rare-gas atoms have been used for investigating new theoretical models for calculating differential electron- and positron-scattering cross sections as well as for calibrating the corresponding experimental measurements. Since 1975, theoretical DCS calculations below the inelastic thresholds (low energy) for *electron-rare-gas* scattering have been presented for helium [3,9–28], neon [24–26,29–37], argon [25,26,38–53], krypton [25,37,51–61], and xenon [25,37,60–65]. DCS calculations for low-energy *positron-rare-gas* scattering have been presented for helium [66–69], neon [70], argon [4,35,49,50,70–73], krypton [73], and xenon [73]. While we have only listed papers in which low-energy DCS calculations were presented, other authors have presented pieces of related information such as the scattering length and the phase shifts in this energy range.

Experimental measurements of differential cross sections, below the first inelastic threshold, for *electron-rare-gas* scattering since 1975 have been

*Permanent address: Department of Physics and Astronomy, Eastern Michigan University, Ypsilanti, MI 48197.

presented for helium [74–83], neon [77,83–86], argon [77,83,87–92], krypton [91–94], and xenon [92,94–97]. Similarly, low-energy DCS measurements for positron–rare-gas scattering have been performed for neon [77], argon [77,98,99], krypton [77,100], and xenon [77].

We remark on the motivation of our work in contrast with the previous calculations. It is to be noted that several of the previous calculations of differential cross sections for the scattering of electrons or positrons from rare gases were carried out for specific targets and, in some instances, might possibly show better agreement with the corresponding experimental data than the present calculations do. In the present work our focus is not necessarily to find the most accurate interaction for any specific electron-atom or positron-atom system. Rather, we strive to obtain a model interaction that would be globally applicable for both electron and positron scattering from different targets.

II. INTERACTION POTENTIALS

We use atomic units unless stated otherwise. In deciding upon the correlation-polarization interaction $V_{cp}(r)$ to be used in the present calculations, we seek a form that satisfies the following reasonable criteria.

(i) V_{cp} behaves asymptotically as

$$-\frac{\alpha_d}{2r^4} - \frac{\alpha_q}{2r^6}$$

as r approaches ∞ . This form is suggested by the classical interaction between a charged projectile and a neutral atom; α_d and α_q are, respectively, the static dipole and quadrupole polarizabilities of the atom.

(ii) For a given projectile-atom system, V_{cp} gets smaller in magnitude as the energy of the projectile increases. This is suggested because intuitively one expects the target atom to experience less distortion from more rapidly moving projectiles due to the reduced response time.

(iii) For a fixed energy of the incident projectile, V_{cp} approaches its asymptotic form more rapidly for smaller atoms. This is expected because the smaller atoms, having fewer electrons, are more tightly bound and are, therefore, more difficult to distort (compare the ionization potentials of various rare-gas atoms, which are 24.588, 21.565, 15.760, 14.000, and 12.130 eV for He, Ne, Ar, Kr, and Xe, respectively).

The above conditions can be satisfied by several forms of V_{cp} , and many were tried in the present investigations. The correlation-polarization interaction that we eventually decided to use has the following form:

$$V_{cp} = -\frac{\alpha_d r^2}{2(r^3 + d^3)^2} - \frac{\alpha_q - (k^2/Z)}{2(r^3 + d^3)^2}, \quad (1)$$

where $E = \hbar^2 k^2 / 2m$ is the energy of the incident projectile and Z is the atomic number of the target atom. The value of the *nonadjustable* parameter d is obtained by setting V_{cp} equal to V_{corr} at the edge of the near-target region where the effects of correlation become important. We define the edge of the near-target region to be located

at the charge-density peak of the outermost occupied orbital; it is sometimes called the orbital radius (R_{orb}). Obtaining d in this manner forces the potential to approximate correlation effects at and inside of R_{orb} . We choose this scheme because explicit use of $V_{corr}(r)$ in the near-target region introduces an undesirable discontinuity in the slope of the total interaction potential at R_{orb} and does not improve the results of our calculations. Also, in this approach the discontinuities in slope arising from piecewise fittings [4,8] of V_{corr} to analytic expressions in different ranges of r are avoided. Figure 1 shows the radial charge density of various rare gases, calculated using analytical Hartree-Fock wave functions [101] that are in the form of Slater determinants made up of normalized one-electron orbitals $\phi_i(\mathbf{r})$. The electron density $\rho(\mathbf{r})$ is given in terms of these one-electron orbitals as

$$\rho(\mathbf{r}) = \sum_{i=1}^Z |\phi_i(\mathbf{r})|^2, \quad (2)$$

with its radial part as

$$\rho(r) = \frac{1}{4\pi} \int \rho(\mathbf{r}) d\Omega. \quad (3)$$

Figure 1 also indicates the approximate location of R_{orb} . Even though the same form is used for both electron and positron projectiles, the correlation-polarization interactions for the two projectiles are different since the V_{corr}

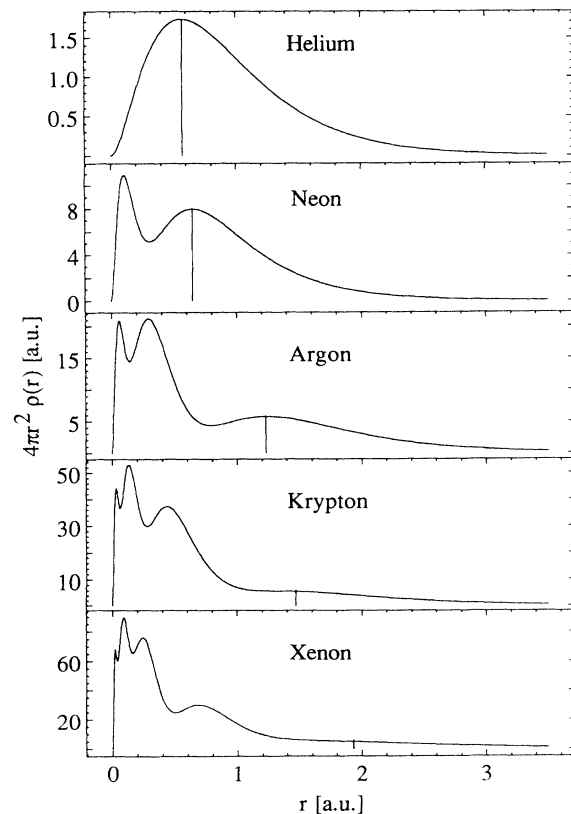


FIG. 1. The radial electron charge density of various rare gases. The vertical line indicates the position of the density peak of the outermost orbital.

TABLE I. Values of α_d , α_q , and R_{orb} for various target atoms as well as the values of the nonadjustable parameter d for both electron and positron impacts.

Target	α_d (a.u.)	α_q (a.u.)	R_{orb} (a.u.)	d (a.u.) for e^+	d (a.u.) for e^-
Helium	1.38	2.44	0.55		1.55–1.6
Neon	2.66	6.42	0.67	1.29	1.86–1.87
Argon	11.1	52.8	1.25	1.84	2.74
Krypton	16.7	95.6	1.50	2.02	3.06
Xenon	27.3	212	1.86	2.28	3.52

used for generating V_{cp} are different. Table I provides the values of α_d , α_q , and R_{orb} for various target atoms as well as the values of the nonadjustable parameter d for both electron and positron scattering in the range of impact energies being presented.

The energy dependence of V_{cp} represents the nonadiabatic correction to the dipole term, which is a measure of the inability of the induced dipole to instantaneously account for the motion of the projectile and is known [102] to behave asymptotically as $1/r^6$. This energy dependence is chosen to be a linear function of k^2 , which is similar to the suggested energy dependence of the nonadiabatic correction to the dipole term [103]. In order to make this correction term different for various target atoms we have explicitly included a Z dependence, which is consistent with criterion (iii) listed above. Figures 2 and 3 show, respectively, correlation-polarization interactions for the scattering of 5-eV electrons and positrons from various rare-gas atoms. The fact that the potential mimics the correlation effects inside of R_{orb} can be seen by observing that the magnitude of V_{cp} in the region

$r \leq R_{\text{orb}}$ is practically the same for any target for electron as well as for positron impact. As noted previously in criterion (iii), one can see clearly in Figs. 2 and 3 that V_{cp} is approaching its asymptotic form more rapidly for smaller atoms. Since the present study is limited to low-energy projectiles, for which k^2 is small, the effect of this term on most of the DCS results presented below is minimal. However, for near threshold scattering from helium and neon targets, for which the inelastic thresholds are relatively high compared to those of argon, krypton, and xenon, we do obtain noticeable improvement at smaller scattering angles ($\theta < 60^\circ$) upon inclusion of the energy dependent term.

The static potential, calculated using electron densities $\rho(r)$, is given by

$$V_s(r) = \frac{Z\varepsilon}{r} - \varepsilon \int \frac{\rho(r')}{|\mathbf{r}-\mathbf{r}'|} d\mathbf{r}', \quad (4a)$$

which for a spherically symmetric density reduces to

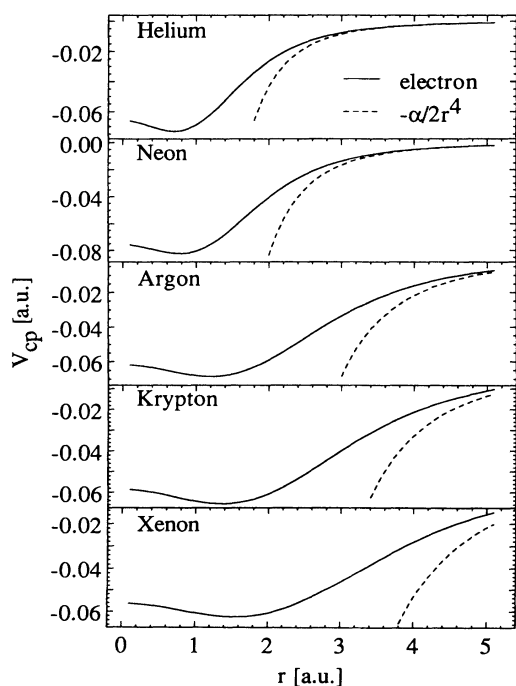


FIG. 2. The correlation-polarization potential, for an incident electron energy of 5 eV, and the dipole asymptotic form ($-\alpha/2r^4$) for various rare-gas atoms.

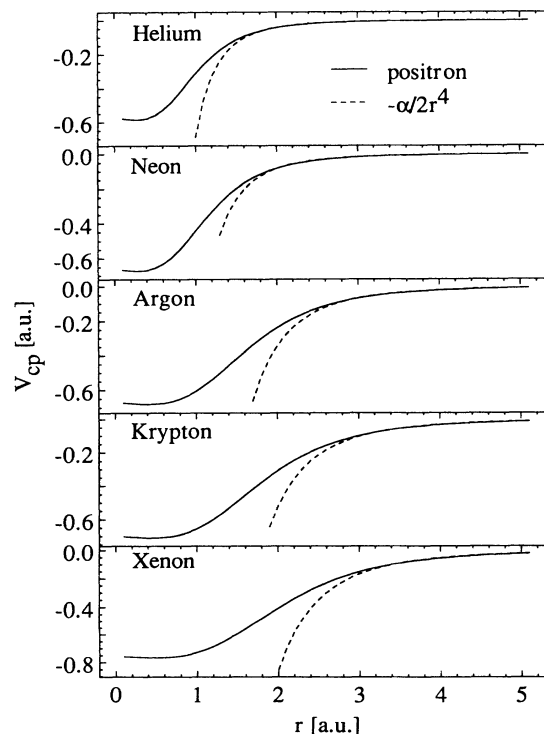


FIG. 3. The correlation-polarization potential, for an incident positron energy of 5 eV, and the dipole asymptotic form ($-\alpha/2r^4$) for various rare-gas atoms.

$$V_s(r) = \frac{Z\varepsilon}{r} - 4\pi\varepsilon \int_{r_>} \frac{\rho(r')}{r} r'^2 dr' . \quad (4b)$$

Here ε is $+1$ for positron projectiles and -1 for electron projectiles. The exchange potential used in the present calculations for closed-shell atoms is given by Riley and Truhlar [104],

$$V_{\text{ex}}(r) = \frac{1}{2} \{ E_D - \sqrt{E_D^2 + 4\pi\rho(r)} \} . \quad (5)$$

In the present case $E_D = E - V_s(r)$.

III. CALCULATIONS

The above potentials are placed in the radial Schrödinger equation and integrated out to a distance of 60 a.u. from the nucleus via the Numerov technique. The first sixteen ($l_{\text{max}} = 15$) phase shifts are calculated exactly by comparing u_l , the radial wave function of the target plus projectile system, at two adjacent points r and $r_+ = r + h$:

$$\tan(\delta_l) = - \frac{r_+ u_l(r) j_l(kr_+) - r u_l(r_+) j_l(kr)}{r u_l(r_+) n_l(kr) - r_+ u_l(r) n_l(kr_+)}, \quad (6)$$

$$f_6(\theta) = -3\pi k^3 \alpha_q \left[-\frac{\sin^3(\theta/2)}{18} + \sum_{l=0}^{l_{\text{max}}} \frac{P_l(\cos\theta)}{(2l+5)(2l+3)(2l-1)(2l-3)} \right], \quad (9)$$

where α_d and α_q are the dipole and quadrupole polarizabilities of the atom, respectively. Finally, the differential cross sections are obtained from the scattering amplitude in the usual manner,

$$\frac{d\sigma}{d\Omega} = |f(\theta)|^2 . \quad (10)$$

IV. RESULTS AND DISCUSSIONS

A. Electron scattering

Previously, we generated [107] complete three-dimensional plots of the DCS surfaces, as functions of the scattering angle and the projectile energy, in the elastic regime for electron scattering from rare gases using correlation-polarization interactions, which were slightly different from the ones used in the present investigations. Even in the present study, we have calculated DCS curves for a very wide range of incident energies below the inelastic thresholds. Figures 4–8, however, display only a few of the present DCS curves for electron scattering from helium, neon, argon, krypton, and xenon. In order to make our figures more clear and intelligible, we compare our theoretical results with only a few selected sets of experimental data.

It is worth noting that helium and neon are distinguished from the other rare gases in that these are relatively small rare-gas atoms and have completely filled shells; the other rare-gas atoms only have filled subshells. (Note that the differences between the excitation as well

where h is the step size (0.00075 a.u.) of the calculation, and j_l and n_l are the spherical Bessel and Neumann functions evaluated using the algorithm of Gillman and Fiebig [105].

The scattering amplitude is obtained by

$$f(\theta) = (2ik)^{-1} \sum_{l=0}^{l_{\text{max}}} (2l+1)(S_l-1)P_l(\cos\theta) + f_4(\theta) + f_6(\theta), \quad (7)$$

where $S_l = \exp(2i\delta_l)$. The functions f_4 and f_6 are the higher l contributions from the Born phase shifts for the dipole ($\sim 1/r^4$) and quadrupole ($\sim 1/r^6$) parts of the polarization potential, respectively. The closed-form expressions, in atomic units, for these functions are [106]

$$f_4(\theta) = -\pi k \alpha_d \left[\frac{\sin(\theta/2)}{2} + \sum_{l=0}^{l_{\text{max}}} \frac{P_l(\cos\theta)}{(2l+3)(2l-1)} \right], \quad (8)$$

and

as ionization energies of argon and neon and of neon and helium are larger than the corresponding differences of xenon and krypton and of krypton and argon.) This suggests that not only are helium and neon more tightly bound atoms because they are smaller, as alluded to in criterion (iii) of Sec. II, but that this binding may be

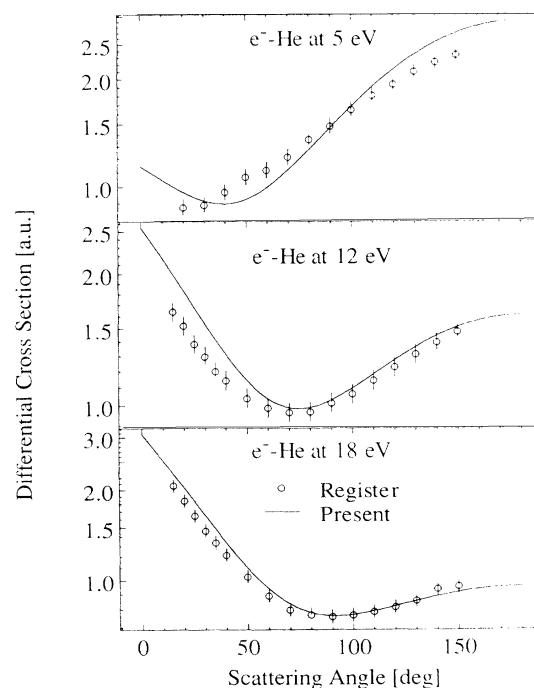


FIG. 4. Differential cross sections for the elastic scattering of 5-, 12-, and 18-eV electrons by helium. The circles (Ref. [74]) are experimental cross sections; the lines are the present results.

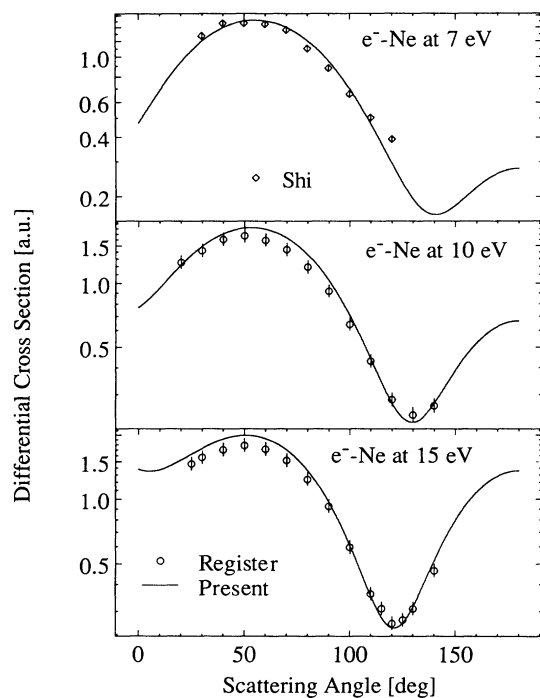


FIG. 5. Differential cross sections for the elastic scattering of 7-, 10-, and 15-eV electrons by neon. The circles (Ref. [85]) and diamonds (Ref. [86]) are experimental cross sections; the lines are the present results.

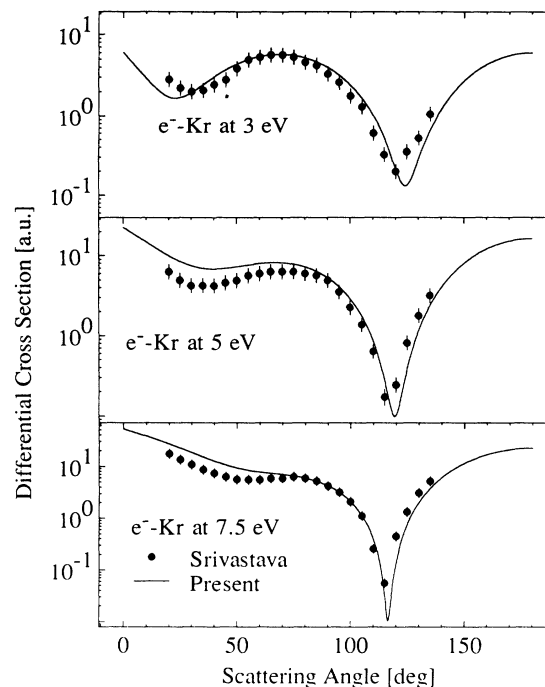


FIG. 7. Differential cross sections for the elastic scattering of 3-, 5-, and 7.5-eV electrons by krypton. The solid circles (Ref. [91]) are experimental cross sections; the lines are the present results.

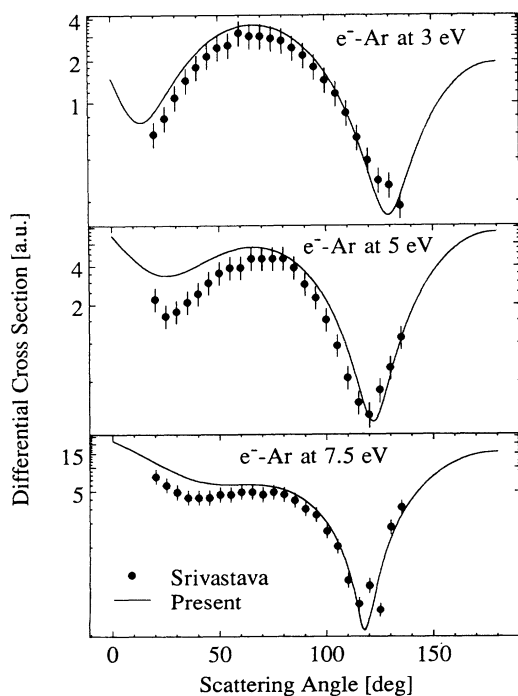


FIG. 6. Differential cross sections for the elastic scattering of 3-, 5-, and 7.5-eV electrons by argon. The solid circles (Ref. [91]) are experimental cross sections; the lines are the present results.

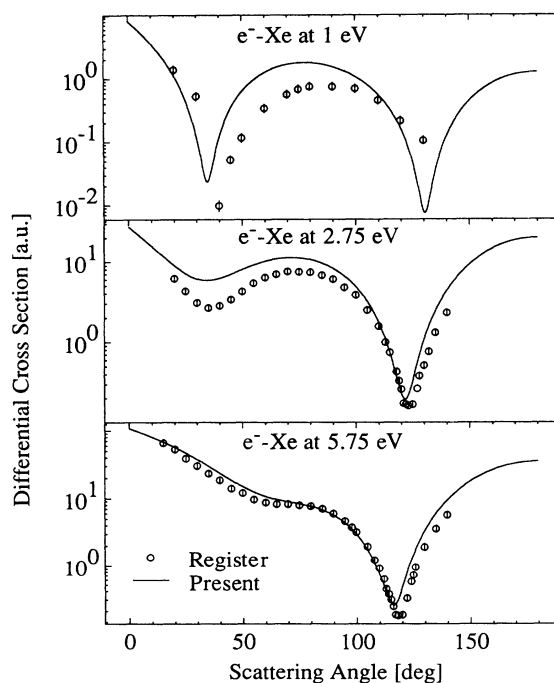


FIG. 8. Differential cross sections for the elastic scattering of 1-, 2.75-, and 5.75-eV electrons by xenon. The circles (Ref. [95]) are experimental cross sections; the lines are the present results.

enhanced due to the fact that these atoms have completely filled shells. Therefore, it is reasonable to believe that it is more important to account for the effects of this stronger binding for helium and neon than for the other rare-gas atoms. This stronger binding suggests a dependence of the correlation-polarization part of the interaction potential on the target Z , which we have taken as in Eq. (1). The fact that the effects of this k^2/Z term are only evident for helium and neon in the present calculations may be explained by the above argument for Z as well as by the increasing influence of k^2 on near threshold scattering from helium and neon targets, for which the inelastic thresholds are relatively high compared to those of argon, krypton, and xenon.

The global picture for electron scattering shows good agreement at larger scattering angles and a tendency to slightly overestimate the differential cross sections at smaller scattering angles for all rare-gas targets. This overestimation, while not too severe, is most pronounced at lower energies and may be partially attributable to the model exchange potential which becomes less accurate at very low energies [104]. More importantly, we note that for all of the targets considered the magnitude and shape of the present DCS curves are quite reliable. The locations of the principal maxima and minima, which are somewhat sensitive to the form of the correlation-polarization interaction used, are consistently predicted with good accuracy. However, in the case of electron-Ar scattering at 3 eV, how well the present calculation fits the second minimum around 130° is ambiguous due to the lack of experimental data above 135° . At 7.5 eV, the present calculation gives good results; however, there is a sharp feature in the experimental data between 120° and 130° . Our calculation does not predict such behavior but produces a curve with this sharp feature smoothed over.

For the electron-Xe cross sections of Fig. 8, we note that the present nonrelativistic calculations can predict the locations of the principal minima in the DCS curves reasonably well, even for this large atom. Furthermore, the accuracy of the calculations improves with increasing electron energy. The xenon DCS curve for 5.75-eV electrons produces one of the best agreements with experimental absolute DCS data among all of our results.

B. Positron scattering

Again, in our previous work, we generated [107], using correlation-polarization interactions which were slightly different from the one used in the present investigations, complete three-dimensional and contour plots of DCS surfaces for positrons scattered from helium, neon, argon, krypton, and xenon as functions of the scattering angle and the projectile energy below the inelastic thresholds. However, in Figs. 9–12 of the present work we compare the DCS curves for positron scattering from Ne, Ar, Kr, and Xe only, using the present interaction potentials, with the available experimental data in the elastic-scattering regime. No DCS curves for the scattering of low-energy positrons from helium are shown since no corresponding experimental data are available. The electron results are better indicators of the quality of the

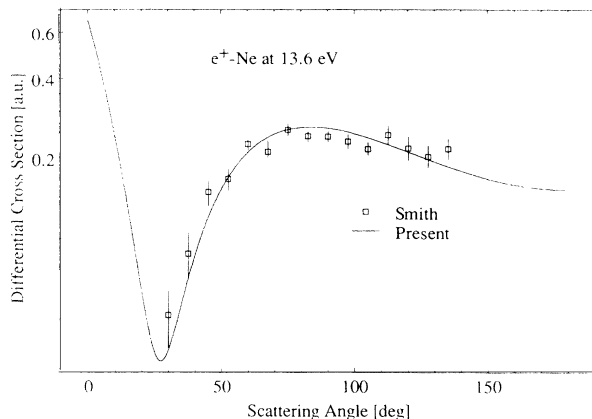


FIG. 9. Differential cross sections for the elastic scattering of 13.6-eV positrons by neon. The squares (Ref. [77]) are experimental cross sections; the line is the present result. The experimental results are normalized to the present calculations at 75° .

correlation-polarization interaction than the positron results; this is because in the case of positron scattering for each target considered, except argon, corresponding experimental data are available at only one incident energy below the inelastic threshold. Furthermore, except for krypton, these experimental differential cross sections are all in the form of relative data requiring some normalization.

As in the electron-scattering case, we find that the shape of the DCS curves and the locations of the minima

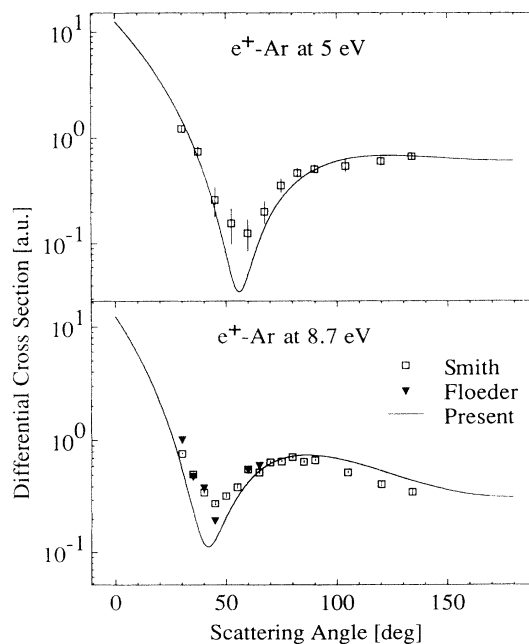


FIG. 10. Differential cross sections for the elastic scattering of 5- and 8.7-eV positrons by argon. The squares (Ref. [77]) and triangles (Ref. [98]) are experimental cross sections; the lines are the present results. The experimental results at 5 and 8.7 eV are normalized to the present calculations at 90° and 70° , respectively.

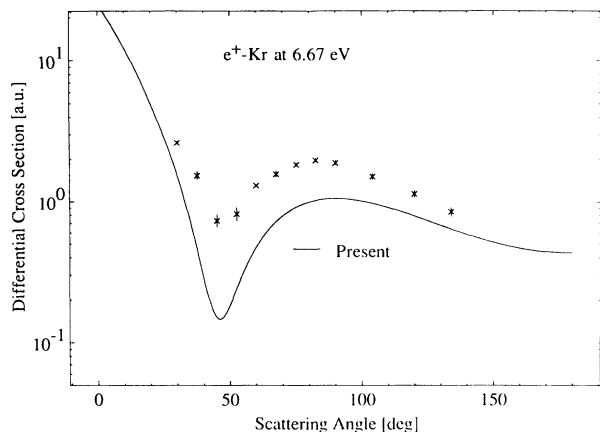


FIG. 11. Differential cross sections for the elastic scattering of 6.67-eV positrons by krypton. The crosses (Ref. [100]) are absolute experimental cross sections; the line is the present result.

are predicted with good accuracy. This fact is particularly important for our goal of obtaining interaction potentials with global applicability because the location of the minima for positron scattering are even more sensitive to the choice of V_{cp} than in the electron case. Even after normalization of the experimental cross sections, our results tend to underestimate the minimum; this underestimation can be partially attributed to the finite angular acceptance of the scattered positron detectors and the finite-energy width of the positron beam (see, for example, Ref. [99]).

Two points concerning the argon and krypton DCS plots are worth noting. In the lower half of Fig. 10, the relative differential cross sections of Floeder *et al.* [98] are at 8.5 eV, whereas the relative cross sections of Smith [77], normalized to the present curve at 70°, and the present calculated cross sections are both at 8.7 eV. In Fig. 11, the present positron-Kr differential scattering cross sections are compared with the absolute experimental data of Dou *et al.* [100]. We see here that the present calculation does provide the overall shape of the DCS

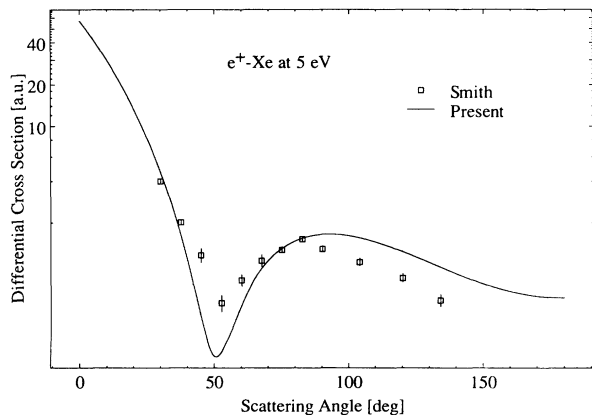


FIG. 12. Differential cross sections for the elastic scattering of 5-eV positrons by xenon. The squares (Ref. [77]) are experimental cross sections; the line is the present result. The experimental results are normalized to the present calculations at 75°.

curve as well as the location of the principal minimum with very good reliability considering the extent to which the actual experimental values overestimate the present calculations. An additional reason for the difference between the experimental results and the present results may be that the experimental errors shown in Fig. 11 are only the statistical uncertainties; the estimated upper limit on the uncertainty, resulting from the normalization procedure used for converting the experimental relative DCS to absolute DCS, is $\pm 20\%$. Since in general the location of the principal minima of the DCS curves is sensitive to the correlation-polarization interaction used in the calculations, it is somewhat surprising that the location of this minimum in the positron-Kr system is predicted so accurately while the DCS curve lies as far below the experimental values as it does.

Although the focus of our investigations is on the calculations of differential cross sections, for the case of positron scattering there are so few measurements of the differential cross sections that a comparison of the present integrated elastic cross sections σ_T , with the corresponding experimental cross sections is worthwhile. However, in several instances the numerical values of the experimental cross sections were not available at exactly the same impact energy E for which the present calculations were done. For comparison purposes, the present theoretical and experimental values of the pair $\{E, \sigma_T\}$ in a.u. are $\{13.6, 2.05\}$ and $\{13.5, 3.40\}$ [108], respectively, for neon; $\{5, 8.94\}$ and $\{5, 9.67\}$ [109], respectively, for argon; $\{6.67, 13.6\}$ and $\{6.8, 17.6\}$ [110], respectively, for krypton; and $\{5, 26.6\}$ and $\{5, 37.5\}$ [110], respectively, for xenon.

V. CONCLUSIONS

We have constructed a correlation-polarization interaction that gives good agreement with low-energy experimental differential cross sections for both electron and positron scattering from all of the rare-gas atoms (there are no experimental data for radon). Even though the results are presented only for a few selected energies of the projectiles, the actual calculations are carried out, for each target atom, over a larger energy range extending from very low to the first inelastic threshold. The correlation-polarization interaction is presented as an analytical expression containing no adjustable parameters. The proposed form of this interaction clearly confirms the importance of accounting for the correlation between the projectile and the target electrons. It is noticed that from among the many models studied, the correlation-polarization interaction that gives good global results also contains, in addition to including correlation effects, dependences on projectile energy (k^2) and on target (Z).

The interactions that we use for electron and positron scattering in the present calculations are identical in analytical form but different in numerical values. The inclusion of correlation effects makes the positron V_{cp} more attractive than the electron V_{cp} in the near-target region (see Figs. 2 and 3). We intend to explore the applicability of this V_{cp} interaction to other atomic target groups (e.g.,

alkali atoms) with our ultimate goal being to obtain a single form of the correlation-polarization interaction that will predict the shape of the differential cross sections for electron and positron scattering from *any atom* with success equal to, or better than, the present calculations for rare gases. Based on the present results, we believe that this goal is achievable, even though this ultimate interaction might require a more complicated dependence on projectile energy and on target. We believe that the

present investigation has brought us closer to achieving this goal.

ACKNOWLEDGMENTS

We gratefully acknowledge the support of NSF (Grant No. PHY91-11870) for this work. We also thank Professor W. E. Kauppila and Professor T. S. Stein for providing useful information.

-
- [1] J. K. O'Connell and N. F. Lane, *Phys. Rev. A* **27**, 1893 (1983).
- [2] N. T. Padial and D. W. Norcross, *Phys. Rev. A* **29**, 1742 (1984).
- [3] Xianzhou Zhang, Jinfeng Sun, and Yufang Liu, *J. Phys. B* **25**, 1893 (1992).
- [4] A. Jain, *Phys. Rev. A* **41**, 2437 (1990).
- [5] K. L. Baluja and A. Jain, *Phys. Rev. A* **46**, 1279 (1992).
- [6] W. J. Carr, Jr. and A. A. Maradudin, *Phys. Rev.* **133**, A371 (1964).
- [7] E. Boronski and R. M. Nieminen, *Phys. Rev. B* **34**, 3820 (1986).
- [8] J. P. Perdew and A. Zunger, *Phys. Rev. B* **23**, 5048 (1981).
- [9] R. P. McEachran and A. D. Stauffer, *J. Phys. B* **16**, 255 (1983).
- [10] T. F. O'Malley, P. G. Burke, and K. A. Berrington, *J. Phys. B* **12**, 953 (1979).
- [11] W. C. Fon, K. A. Berrington, and A. Hibbert, *J. Phys. B* **14**, 307 (1981).
- [12] H. P. Saha, *Phys. Rev. A* **40**, 2976 (1989).
- [13] I. Khurana, R. Srivastava, and A. N. Tripathi, *Phys. Rev. A* **37**, 3720 (1988).
- [14] A. S. Ghosh, C. Falcon, and D. Bhattacharya, *J. Phys. B* **14**, 4619 (1981).
- [15] P. Khan, S. Datta, D. Bhattacharya, and A. Ghosh, *Phys. Rev. A* **29**, 3129 (1984).
- [16] T. W. Shyn, *Phys. Rev. A* **22**, 916 (1980).
- [17] R. C. Dehmel, M. A. Fineman, and D. R. Miller, *Phys. Rev. A* **13**, 115 (1976).
- [18] M. Gryzinski and M. Kowalski, *Fizika (Zagreb)* **19**, 135 (1987).
- [19] B. Plenkiewicz, P. Plenkiewicz, and J. P. Jay-Gerin, *Can. J. Phys.* **68**, 104 (1990).
- [20] M. J. Brunger, S. J. Buckman, L. J. Allen, I. E. McCarthy, and K. Ratnavelu, *J. Phys. B* **25**, 1823 (1992).
- [21] D. E. Golden, J. Furst, and M. Mahgerefteh, *Phys. Rev. A* **30**, 1247 (1984).
- [22] R. I. Campeanu, *Z. Phys. A* **320**, 579 (1985).
- [23] R. K. Nesbet, *Phys. Rev. A* **20**, 58 (1979).
- [24] F. Kemper, F. Rosicky, and R. Feder, *J. Phys. B* **17**, 3763 (1984).
- [25] K. Ohya and I. Mori, *Jpn. J. Appl. Phys.* **29**, 2145 (1991).
- [26] F. A. Gianturco and J. A. Rodriguez-Ruiz, *Phys. Rev. A* **47**, 1075 (1993).
- [27] H. P. Saha, *Phys. Rev. A* **48**, 1163 (1993).
- [28] D. De Fazio, F. A. Gianturco, J. A. Rodriguez-Ruiz, K. T. Tang, and J. P. Toennies, *J. Phys. B* **27**, 303 (1994).
- [29] H. P. Saha, *Phys. Rev. A* **39**, 5048 (1989).
- [30] W. C. Fon and K. A. Berrington, *J. Phys. B* **14**, 323 (1981).
- [31] A. Dasgupta and A. K. Bhatia, *Phys. Rev. A* **30**, 1241 (1984).
- [32] T. Suzuki, H. Tanaka, M. Saito, and H. Igawa, *J. Phys. Soc. Jpn.* **39**, 195 (1975).
- [33] H. P. Berg, *J. Phys. B* **15**, 3769 (1982).
- [34] L. Fritsche, J. Noffke, and H. Gollisch, *J. Phys. B* **17**, 1637 (1984).
- [35] H. Nakanishi and D. Schrader, *Phys. Rev. A* **34**, 1823 (1986).
- [36] R. P. McEachran and A. D. Stauffer, *J. Phys. B* **16**, 4023 (1983).
- [37] R. Haberland, L. Fritsche, and J. Noffke, *Phys. Rev. A* **33**, 2305 (1986).
- [38] H. P. Saha, *Phys. Rev. A* **43**, 4712 (1991).
- [39] B. Plenkiewicz, P. Plenkiewicz, and J. P. Jay-Gerin, *Phys. Rev. A* **38**, 4460 (1988).
- [40] B. Plenkiewicz, P. Plenkiewicz, P. Baillargeon, and J. P. Jay-Gerin, *Phys. Rev. A* **36**, 2002 (1987).
- [41] S. Datta, S. K. Mandal, P. Khan, and A. Ghosh, *Phys. Rev. A* **31**, 633 (1985).
- [42] M. Ya. Amusia, N. A. Cherepkov, L. V. Chernysheva, D. M. Davidovic, and V. Radojevic, *Phys. Rev. A* **25**, 219 (1982).
- [43] K. R. Karim and A. Jain, *Phys. Scr.* **39**, 238 (1989).
- [44] H. P. Saha, *Phys. Rev. A* **47**, 273 (1993).
- [45] J. E. Bloor and R. E. Shrood, *J. Phys. Chem.* **90**, 5508 (1986).
- [46] J. E. Sienkiewicz and W. E. Baylis, *J. Phys. B* **20**, 5145 (1987).
- [47] S. Y. Yousif and J. A. D. Matthew, *J. Phys. B* **19**, 3305 (1986).
- [48] K. L. Bell, N. S. Scott, and M. A. Lennon, *J. Phys. B* **17**, 4757 (1984).
- [49] S. N. Nahar and J. M. Wadehra, *Phys. Rev. A* **35**, 2051 (1987).
- [50] S. N. Nahar and J. M. Wadehra, *Phys. Rev. A* **43**, 1275 (1991).
- [51] H. P. Berg, *Physica* **122B&C**, 129 (1983).
- [52] F. Kemper, B. Awe, F. Rosicky, and R. Feder, *J. Phys. B* **16**, 1819 (1983).
- [53] D. J. R. Mimmagh, R. P. McEachran, and A. D. Stauffer, *J. Phys. B* **26**, 1727 (1993).
- [54] W. C. Fon, K. A. Berrington, and A. Hibbert, *J. Phys. B* **17**, 3279 (1984).
- [55] D. Basu, S. K. Datta, P. Khan, and A. S. Ghosh, *Phys. Rev. A* **35**, 5255 (1987).
- [56] B. Plenkiewicz, P. Plenkiewicz, C. Houee-Levin, and J. P. Jay-Gerin, *Phys. Rev. A* **38**, 6120 (1988).
- [57] K. L. Baluja, A. Jain, H. W. Jones, C. A. Weatherford, and A. Amaya-Tapia, *Phys. Scr.* **45**, 30 (1992).
- [58] J. E. Sienkiewicz and W. E. Baylis, *J. Phys. B* **25**, 2081 (1992).

- (1992).
- [59] K. L. Bell, K. A. Berrington, and A. Hibbert, *J. Phys. B* **21**, 4205 (1988).
- [60] J. Yuan and Z. Zhang, *J. Phys. B* **22**, 2581 (1989).
- [61] R. P. McEachran and A. D. Stauffer, *J. Phys. B* **17**, 2507 (1984).
- [62] H. P. Berg, *Phys. Lett.* **88A**, 292 (1982).
- [63] J. E. Sienkiewicz and W. E. Baylis, *J. Phys. B* **22**, 3733 (1989).
- [64] W. Jaskolski, J. Karwowski, and J. Kobus, *Phys. Scr.* **36**, 436 (1987).
- [65] J. Yuan and Z. Zhang, *J. Phys. B* **24**, 275 (1991).
- [66] I. Khurana, R. Srivastava, and A. N. Tripathi, *Phys. Rev. A* **37**, 3720 (1988).
- [67] I. Khurana and R. Srivastava, *Phys. Rev. A* **37**, 3580 (1988).
- [68] P. Khan, S. Datta, D. Bhattacharya, and A. Ghosh, *Phys. Rev. A* **29**, 3129 (1984).
- [69] T. L. Gibson, *J. Phys. B* **23**, 767 (1990).
- [70] F. A. Gianturco, A. Jain, and J. A. Rodriguez-Ruiz, *Phys. Rev. A* **48**, 4321 (1993).
- [71] J. E. Sienkiewicz and W. E. Baylis, *Phys. Rev. A* **40**, 3662 (1989).
- [72] S. Datta, S. K. Mandal, P. Khan, and A. Ghosh, *Phys. Rev. A* **31**, 633 (1985).
- [73] J. M. Wadehra, T. S. Stein, and W. E. Kauppila, *Phys. Rev. A* **29**, 2912 (1984).
- [74] D. F. Register, S. Trajmar, and S. K. Srivastava, *Phys. Rev. A* **21**, 1134 (1980).
- [75] D. Andrick and A. Bitsch, *J. Phys. B* **8**, 402 (1975).
- [76] R. W. Wagenaar, A. de Boer, T. van Tubergen, J. Los, and F. J. de Heer, *J. Phys. B* **19**, 3121 (1986).
- [77] S. J. Smith, Ph. D. thesis, Wayne State University, Detroit (1989).
- [78] N. R. Newell, D. F. C. Brewer, and A. C. H. Smith, *J. Phys. B* **14**, 3209 (1981).
- [79] M. M. Arnou, *Phys. Rev. A* **10**, 1223 (1974).
- [80] J. W. McConkey and J. A. Preston, *J. Phys. B* **8**, 63 (1975).
- [81] P. N. Tsung, *Physica* **79B&C**, 520 (1975).
- [82] S. K. Srivastava and S. Trajmar, *J. Chem. Phys.* **64**, 3886 (1976).
- [83] J. F. Williams, *J. Phys. B* **12**, 265 (1979).
- [84] D. F. C. Brewer, W. R. Newell, S. F. W. Harper, and A. C. H. Smith, *J. Phys. B* **14**, L749 (1981).
- [85] D. F. Register and S. Trajmar, *Phys. Rev. A* **29**, 1785 (1984).
- [86] X. Shi and P. D. Burrow, *J. Phys. B* **25**, 4273 (1992).
- [87] J. E. Furst, D. E. Golden, M. Mahgerefteh, J. Zhou, and D. Mueller, *Phys. Rev. A* **40**, 5592 (1989).
- [88] Z. Qing, M. J. M. Beerlage, and M. J. van der Wiel, *Physica* **113B&C**, 225 (1982).
- [89] D. M. Filipovic, M. S. thesis, Institute of Physics, Beograd, 1984.
- [90] P. G. Coleman, J. D. McNutt, J. T. Hutton, L. M. Diana, and J. L. Fry, *Rev. Sci. Instrum.* **51**, 935 (1980); P. G. Coleman and J. D. McNutt, *Phys. Rev. Lett.* **42**, 1130 (1979).
- [91] S. K. Srivastava, H. Tanaka, A. Chutjian, and S. Trajmar, *Phys. Rev. A* **23**, 2156 (1981).
- [92] M. Weyhewrwe, B. Barzick, A. Mann, and F. Linder, *Z. Phys. D* **7**, 333 (1988).
- [93] A. Danjo, *J. Phys. B* **21**, 3759 (1988).
- [94] T. Heindorff, J. Hoff, and P. Dabkiewicz, *J. Phys. B* **9**, 89 (1976).
- [95] D. F. Register, L. Vuskovic, and S. Trajmar, *J. Phys. B* **19**, 1685 (1986).
- [96] M. Klewer, M. J. M. Beerlage, and M. J. van der Wiel, *J. Phys. B* **13**, 571 (1980).
- [97] H. Nishimura, T. Matsuda, and A. Danjo, *J. Phys. Soc. Jpn.* **56**, 70 (1987).
- [98] K. Floeder, P. Honer, W. Raith, A. Schwab, G. Sinapius, and G. Spicher, *Phys. Rev. Lett.* **60**, 2363 (1988).
- [99] S. J. Smith, G. M. A. Hyder, W. E. Kauppila, C. K. Kwan, and T. S. Stein, *Phys. Rev. Lett.* **64**, 1227 (1990).
- [100] L. Dou, W. E. Kauppila, C. K. Kwan, D. Przybyla, S. J. Smith, and T. S. Stein, *Phys. Rev. A* **46**, R5327 (1992).
- [101] E. Clementi and C. Roetti, *At. Data Nucl. Data Tables* **14**, 177 (1974).
- [102] C. J. Kleinman, Y. Hahn, and L. Spruch, *Phys. Rev.* **165**, 53 (1968).
- [103] M. J. Seaton and L. Steenman-Clark, *J. Phys. B* **10**, 2639 (1977).
- [104] M. E. Riley and D. G. Truhlar, *J. Chem. Phys.* **63**, 2182 (1975).
- [105] E. Gillman and H. R. Fiebig, *Comput. Phys.* **2**, 62 (1988).
- [106] J. M. Wadehra and S. N. Nahar, *Phys. Rev. A* **36**, 1458 (1987).
- [107] D. D. Reid and J. M. Wadehra, *Hyperfine Int.* **89**, 435 (1994).
- [108] T. S. Stein, W. E. Kauppila, V. Pol, J. H. Smart, and G. Jesion, *Phys. Rev. A* **17**, 1600 (1978).
- [109] W. E. Kauppila, T. S. Stein, and G. Jesion, *Phys. Rev. Lett.* **36**, 580 (1976).
- [110] M. S. Dababneh, W. E. Kauppila, J. P. Downing, F. Laperriere, V. Pol, J. H. Smart, and T. S. Stein, *Phys. Rev. A* **22**, 1872 (1980).